Proceedings of
2001 ASME International Mechanical Engineering Congress and Exposition
November 11-16, 2001, New York, NY

IMECE2001/MEMS-23813

A CMOS-MEMS Micromirror With Large Out-of-Plane Actuation

Huikai Xie[1], Yingtian Pan[3,4] and Gary K. Fedder[1,2]
[1]Dept of Electrical and Computer Engineering; [2]The Robotics Institute; [3]Science and Technology Center
Carnegie Mellon University, Pittsburgh, PA 15213, USA
[4]Departments of Medicine and Bioengineering
University of Pittsburgh, 3550 Terrace Street, Pittsburgh, PA 15261
Email: xie@ece.cmu.edu; pany@msx.dept-med.pitt.edu; fedder@ece.cmu.edu

ABSTRACT

This paper reports a high-aspect-ratio, silicon-based vertical comb drive used to actuate a micromirror. The large displacement is achieved by the curled-up comb drives. This high-aspect-ratio vertical comb drive uses the vertical capacitance gradient of the sidewall capacitor existing between comb fingers. The electrical isolation is realized by using the undercut of the deep Si etch. The 1 mm by 1 mm micromirror is made of an approximately 40 μm-thick single-crystal silicon membrane with aluminum coated on the surface. The mirror has a peak-to-peak curling of 0.5 μm. The mechanical rotation angle of the mirror is ±5°. The fabrication process is compatible with standard CMOS processes, and there is no need for wafer bonding and accurate front-to-backside alignment. Such capability has potential applications in optical switches, optical scanners, interferometric systems, and vibratory gyroscopes.

Key words: micromirror, curled comb drive, high-aspect-ratio

INTRODUCTION

Micromirrors have obtained extensive attention recently because of their applications in optical switches and displays. They are also used in a wide range of other applications, such as interferometric systems, optical spectroscopy, aberration correction and medical imaging. The requirements of micro-mirrors vary with different applications. For optical displays, fill factor and pixel size are the most important parameters. For optical switches, speed, reflectivity, maximum tilt angle and power consumption are primary requirements. The primary application for the work reported here is in endoscopic optical coherence tomography as a noninvasive technique to image tissue morphology at nearly the resolution of histology [Feldchtein et al., 1998]. The required micromirror specifications are a 1 mm^2 surface area and a ±5° scanning range.

Micromirrors have been demonstrated by using different micromachining processes. A successful example of surface-micromachined micromirrors is Texas Instruments's digital mirror devices (DMDs) [Hornbeck 1993]. However, the surface micromachining has difficulty in achieving large mirrors with large tilt range. Bulk-micromachining processes have been used to make sidewall mirrors [Juan and Pang 1998], but the sidewall angle and smoothness are concerns and this type of mirrors is not area-efficient. Another choice is to combine surface- and bulk- micromachining processes. A research group at UC-Berkeley reported a single-crystal silicon (SCS) based micromirror by using silicon-on-insulator (SOI) wafers and two-side alignment [Conant et al. 2000]. A UCLA group assembled an SCS mirror on top of polysilicon actuators [Su et al. 2001].

In this paper, we present a CMOS-MEMS mirror that has a new type of electrostatic comb drive that can generate large displacement. The mirror is made of single-crystal silicon (SCS) and coated with aluminum. A deep reactive-ion-etch (DRIE) CMOS-MEMS process [Xie et al. 2000] is employed. The micromachining process steps are performed after the foundry CMOS process steps are completed, and are completely compatible with conventional CMOS processes. Unlike the commonly-used lateral comb drives, the stator and rotor comb fingers of our new comb drive do not lie in the same plane, and therefore large electrically actuated displacement is achieved.

The DRIE CMOS-MEMS process is briefly introduced first. Next, the concept and principle of the curled comb drive and electrical isolation of silicon are discussed in detail. Then measurement results validating the operation are presented.

DRIE CMOS-MEMS process

It is well known that thin-film deposition processes generate residual stress and stress gradients which cause curling. This curling limits the useful size of micromirrors. The small gap generated by the sacrificial layer present in surface-micromachined mirrors restricts their tilt range. In order to overcome some of the drawbacks of thin-film microstructures, a new process called the DRIE CMOS-MEMS process, has been developed [Xie et al. 2000]. It is a modified version of a previous thin-film CMOS-MEMS process [Fedder et al. 1996]. The basic idea is to introduce a single-crystal silicon (SCS) layer underneath the CMOS multi-layer structures in such a way that the mechanical properties are dominated by the SCS layer and electrical connections are provided by the CMOS interconnect metal layers. A backside etch is used to eliminate the remaining silicon substrate under the microstructures. Therefore, the microstructures can theoretically move hundreds of microns.

The process flow is given in Fig. 1. We start with a deep anisotropic backside etch leaving a 10 to 100 µm thick SCS membrane (Fig. 1(a)). This backside etch step is used to control the thickness of microstructures as well as to form a cavity to simplify the packaging process. Next an anisotropic dielectric etch is performed from the frontside (Fig. 1(b)), followed by a deep silicon etch (Fig. 1(c)). Therefore, a thick SCS layer remains underneath the CMOS layer, resulting in a very flat released microstructure. Finally, a brief isotropic silicon etch is performed (Fig. 1(d)). Any beam with a half-width less than the silicon undercut will have no SCS layer underneath. This type of beam can be used to form electrically isolated SCS islands, curled-up structures and z-compliant springs.

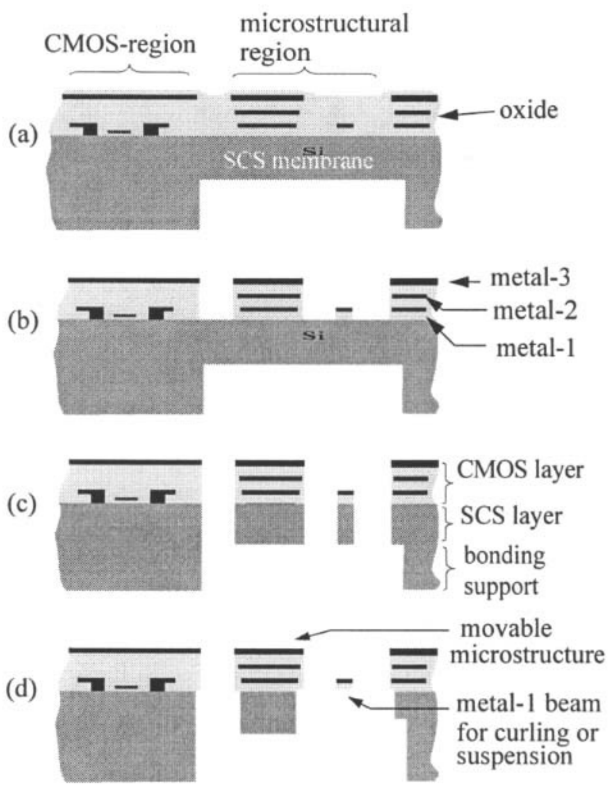

Figure 1. The process-flow for DRIE CMOS-MEMS micromachining. (a) CMOS-chip with backside etch. (b) Anisotropic oxide etch. (c) Deep silicon etch. (d) Isotropic silicon undercut.

Curled comb drive

The metal-1 beam shown in Fig. 1(d) has only thin layers of interconnect aluminum and dielectrics. The beam curls up after it is released because of the residual stress and different coefficients of thermal expansion of the embedded materials [Lu et al. 1998]. Thus, a comb drive with the stationary and movable fingers at different levels, *i.e.*, a curled comb drive, can be created. The concept of the curled-up comb drive is illustrated in Fig. 2. The comb drive has two parts: a set of tilted comb-fingers and a set of flat comb-fingers. The tilted comb-fingers are composed of a curled metal-1 mesh and an array of tilted comb fingers with a thick SCS layer. The silicon substrate underneath the metal-1 mesh is completely undercut during the deep Si etch because the metal-1 mesh consists of only narrow beams. Therefore, the SCS chunks under the tilted comb fingers are electrically isolated from the silicon substrate. The SCS chunks then can be wired to any place on the chip, *e.g.*, a bonding pad. When a voltage is applied to the comb drive, the tilted comb-fingers will tend to align with the flat comb-fingers or vice versa and thus a rotation is generated. The tilt angle of the curled comb-fingers depends on the length of the metal-1 mesh and can be 45° or even larger. So large rotation angle can be expected.

Z-compliant spring

The same technique is applied to the z-spring beams to obtain thin structures that are very compliant in the z-direction. These z-spring beams are constructed from narrow beams, so that the silicon substrate underneath is completely undercut. It has been shown that the curled beams significantly lower the resonant frequency ratio of the primary rotational mode over the z-mode [Xie and Fedder 2001].

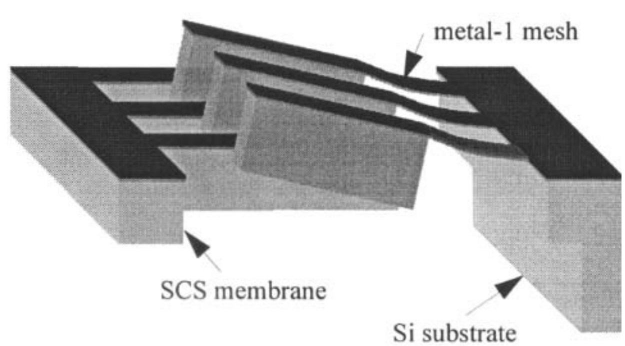

Figure 2. Schematic of a curled-up comb drive.

SCS MICROMIRROR

The device is fabricated in the Hewlett-Packard 3-metal 0.5 μm CMOS process followed by the DRIE CMOS-MEMS micromachining process. The top view of a released device is shown in Fig. 3(a). The mirror is 1mm by 1mm. A curled comb attached to the center plate will pull the center plate down; while a curled comb anchored on the substrate will lift the center plate up. There are eight curled comb drives. The arrangement is chosen such that the center plate can be rotated up on the right as well as on the left. The comb pairs 1A and 1B generate torques in the same direction and cancel each other's z-axis forces. The same arrangement is applied in design of the other three comb pairs. The comb pairs 1A/1B and 1A'/1B' rotate the mirror clockwise, and 2A/2B and 2A'/2B' rotate the mirror counterclockwise.

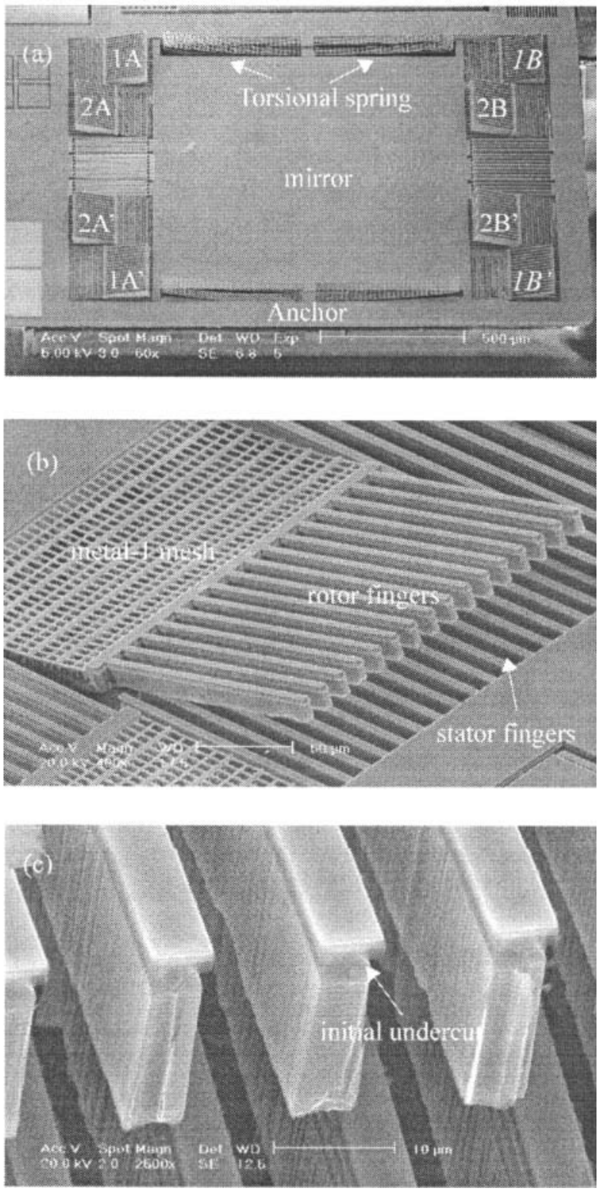

Figure 3. SEMs of the released device. (a) Top view (b) A curled-up comb drive. (c) Close-up of the curled beams.

A view of a curled comb is shown in Fig. 3(b). The lengths of the metal-1 mesh and the SCS fingers are 120 μm and 150 μm, respectively. The thickness of the SCS chunks is about 40 μm. Fig. 3(c) is a close-up of the comb fingers. A small initial undercut is used to assure the complete undercut of silicon underneath the metal-1 meshes and z-compliant springs. To further guarantee the electrical isolation of the silicon chunks, an n-doped well (with p-substrate) is placed underneath the metal-1 meshes and z-compliant springs. The electrical isolation was achieved from all of the tested devices.

CHARACTERIZATION

The profile of the mirror surface was characterized by using a Wyko NT2000 3D Optical Profiler. The measured peak-to-peak curling across the entire mirror is 0.5 μm (Fig. 4). This curling can be reduced by using just metal-1 on the top of the SCS layer or simply increasing the thickness of the SCS layer. Both static and dynamic responses of the device have been tested. Fig. 5 shows the rotation angle versus the applied voltage. By applying 18 V, a tilt of 4.7° can be obtained. Since the width of the entire device is 1.5 mm, the z-displacement at the comb-finger tips is 62 μm. The center plate can rotate to

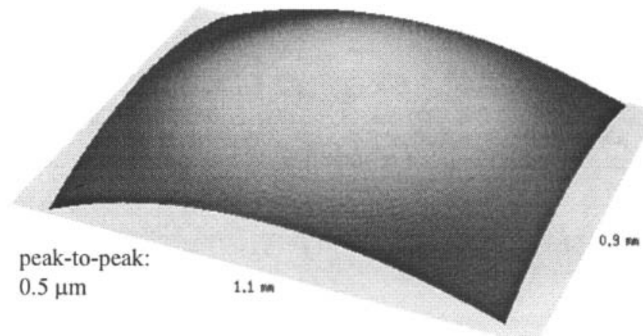

Figure 4. Contour plot of the mirror profile.

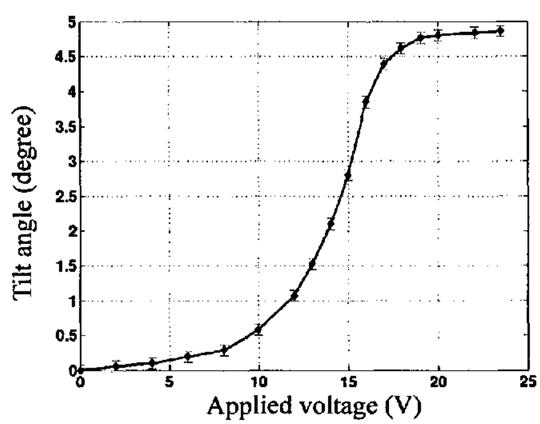

Figure 5. The mirror rotation angle versus applied voltage.

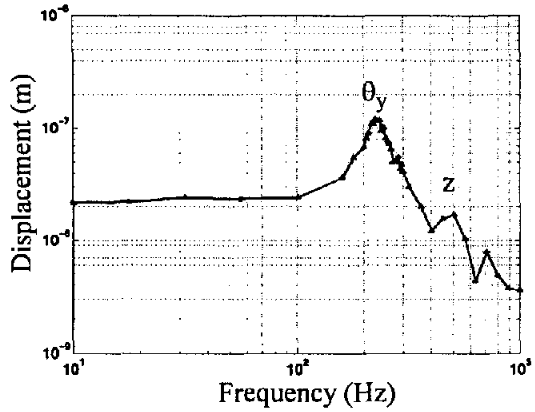

Figure 6. Frequency response measured by using an optical microvision system.

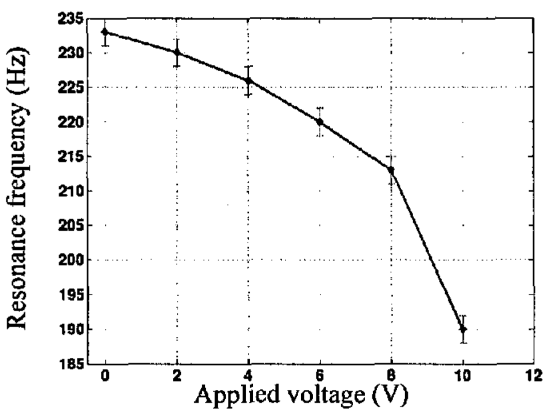

Figure 7. Electrostatic spring "softening" effect.

both sides and therefore a total rotation angle of 9.4° can be achieved. The rotation angle saturates above 20 V. The frequency response measured by using an optical microvision system [Hemmert et al. 1999] is plotted in Fig. 6. The resonant frequency is 233 Hz. An electrostatic spring "softening" effect is also observed in this vertical comb drive, as shown in Fig. 7.

CONCLUSIONS and FUTURE WORK

A large, flat micromirror with large out-of-plane actuation has been experimentally demonstrated. The 9.4° rotation angle of the 1 mm by 1 mm mirror resulted from an initial design. The mirror topology can be optimized for larger rotation angle or larger size. For example, by simply moving the curled comb drives from the two sides to the two ends and closer to the central axis, much larger rotation angle will be achieved. The mirror has potential applications in optical switches, optical scanners, interferometric systems and medical imaging.

The curled comb drive proposed in this paper works very well. More detailed simulation and possible applications are under investigation.

ACKNOWLEDGMENTS

This work was sponsored by DARPA under the AFRL, Air Force Materiel Command, USAF, under agreement F30602-97-2-0323 (GKF) and from NIH 1R01DK059265-01 (YP) and the Whitaker Foundation (YP).

REFERENCES

Hornbeck, L.J., 1993, "Current status of the digital micromirror device (DMD) for projection television applications," *Technical Digest. International Electron Devices Meeting*, Washington, DC, pp. 381 -384.

Juan W.-H. and Pang S.W., 1998, "High-aspect-ratio Si vertical micromirror arrays for optical switching," *Journal of Microelectromechanical Systems*, vol. 7, pp.207-213.

Conant R., Nee J., Lau K. and Muller R., 2000, "A flat high-frequency scanning micromirror," *Technical Digest. 2000 Solid-State Sensor & Actuator Workshop*, Hilton Head, SC, pp.6-9.

Su, G.-D., Toshiyoshi, H. and Wu, M.C., 2001, "Surface-micromachined 2-D optical scanners with high-performance single-crystalline silicon micromirrors," *IEEE Photonics Technology Letters*, vol. 13, pp. 606-608.

Xie H., Erdmann L., Zhu X., Gabriel K. and Fedder G. K., 2000, "Post-CMOS processing for high-aspect-ratio integrated silicon microstructures," *Technical Digest. 2000 Solid-State Sensor & Actuator Workshop*, Hilton Head, SC, pp.78-81.

Fedder G. K., Santhanam S., Reed M., Eagle S., Guillou D., Lu M. and Carley L.R., 1996, "Laminated high-aspect-ratio microstructures in a conventional CMOS process," *Sensors and Actuators A*, vol.A57, pp.103-110.

Lu M., Zhu X. and Fedder G. K., 1998, "Mechanical property measurement of 0.5-μm CMOS microstructures," *Symposium on Microelectromechanical Structures for Materials Research*, San Francisco, CA, pp.27-32.

Xie H. and Fedder G. K., 2001, "A CMOS-MEMS lateral-axis gyroscope," *Technical Digest of the 14th IEEE International Conference on Micro Electro Mechanical Systems (MEMS 2001)*, Interlaken, Switzerland, pp. 162-165.

Hemmert W., Mermelstein M. and Freeman D., 1999, "Nanometer resolution of 3-D motions using video interference microscopy," *Technical Digest of the 12th IEEE International Conference on Micro Electro Mechanical Systems (MEMS'99)*, Orlando, FL, pp. 302-308.

Feldchtein F. I., Sergeev A. M. et al., 1998, "Endoscopic applications of optical coherence tomography," *Optics Express* vol. 3, no. 6, pp. 257-270.